ADVANCED MATERIALS

nanotube is observed and the lower side of the wall corresponds to the outside of the nanotube. The thickness of the wall is about 3.3 nm and it consists of many parallel graphene layers. Each layer, however, curves and wrinkles to some extent, indicating lower crystallinity of the present nanotubes than the ones prepared by other methods, such as arc discharge synthesis. It should be noted that this image does not exhibit any clear difference in crystallinity between pure carbon layers (upper half of the wall) and N-doped layers (the lower half). In the case of nanotubes from P-A CVD, their HRTEM images (not shown here) were found to be very similar to the image of Figure 4, and again there was no crystallinity difference between N-doped and undoped multiwalls.

In conclusion, this study has demonstrated the fabrication of aligned carbon nanotubes with double coaxial structure of N-doped and undoped multiwalls. It can be determined whether the N-doped layer belongs to the inner or outer multiwalls by changing the sequence of the two-step CVD process. Moreover, the thickness of both the N-doped and pure carbon layers is controllable by changing each CVD period. The use of the AAO film as a template enables us for the first time to precisely control the nitrogen location in N-doped carbon nanotubes. Since nitrogen doping would enhance the electron-conducting properties of carbon nanotubes, the present carbon nanotubes may exhibit excellent performance as field electron emitters. The present technique opens up a novel route for the synthesis of heteroatom-doped carbon nanotubes with double coaxial structure and furthermore this will lead to the production of coaxial heterojunctions (pn, npn, or pnp) by stacking N- and B-doped layers.

Experimental

By anodic oxidation of an aluminum plate, an AAO film with a channel diameter of 30 nm and a thickness of about 70 μm was prepared. Details are given elsewhere [13]. The resultant AAO film was placed on a quartz boat in a horizontal quartz reactor (inside diameter 55 mm). The reactor temperature was then increased to 800 °C under N_2 flow. When the temperature reached 800 °C, propylene gas (1.2 % in N_2) was passed through the reactor at a total flow rate of 1000 cm^3(STP)/min. After the 2 h carbon deposition from propylene, the reactor was cooled down to room temperature and the carbon-coated AAO film taken out. In the second step, the carbon-coated film was placed in the reactor again and acetonitrile vapor (4.2 % in N_2 of 500 cm^3(STP)/min) was allowed to flow over the film at 800 °C. The vapor was generated by bubbling N_2 through acetonitrile liquid in a saturator kept at 0 °C. This acetonitrile CVD was performed for 5 h. After this two-step sequential CVD process, the doubly coated AAO film was treated with 10 M NaOH solution at 150 °C for 6 h to remove the alumina template, thereby liberating the nanotubes from the template AAO film.

The carbon-coated AAO films and the corresponding carbon nanotubes were analyzed by X-ray photoelectron spectroscopy (XPS). The samples were mounted on a stainless steel sample holder (6 mm diameter) with silver paste. Carbon and nitrogen 1s (C 1s and N 1s) spectra were recorded using a Shimadzu ESCA 750 spectrometer with Mg Kα radiation (8 kV, 30 mA) under a pressure of less than 5×10^{-6} Pa. Each spectrum was scanned 50 times with 0.05 and 0.1 eV step energy for C 1s and N 1s, respectively. For both the cases, the sampling time for each step energy was 200 ms. An energy correction was made to account for sample charging based on the Ag 3d peak at 367.9 eV. The carbon and nitrogen contents were analyzed by ultimate analysis of the carbon nanotubes. The microscopic features of the carbon nanotubes were observed by TEM (JEOL JEM-2010) and SEM (JEOL, JSM-5400F).

Received: December 16, 2002
Final version: March 15, 2003

[1] M. Yudasaka, R. Kikuchi, Y. Ohki, S. Yokomura, *Carbon* **1997**, *35*, 195.
[2] K. Suenaga, M. Yudasaka, C. Colliex, S. Iijima, *Chem. Phys. Lett.* **2000**, *316*, 365.
[3] R. Sen, B. C. Satishkumar, A. Govindaraj, K. R. Harikumar, G. Raina, J. P. Zhang, A. K. Cheetham, C. N. R. Rao, *Chem. Phys. Lett.* **1998**, *287*, 671.
[4] M. Nath, B. C. Satishkumar, A. Govindaraj, C. P. Vinod, C. N. R. Rao, *Chem. Phys. Lett.* **2000**, *322*, 333.
[5] M. Terrones, P. Redlich, N. Grobert, S. Trasobares, W. K. Hsu, H. Terrones, Y. Q. Zhu, J. P. Hare, C. L. Reeves, A. K. Cheetham, M. Rühle, H. W. Kroto, D. R. M. Walton, *Adv. Mater.* **1999**, *11*, 655.
[6] M. Terrones, H. Terrones, N. Grobert, W. K. Hsu, Y. Q. Zhu, J. P. Hare, H. W. Kroto, D. R. M. Walton, P. Kohler-Redlich, M. Rühle, J. P. Zhang, A. K. Cheetham, *Appl. Phys. Lett.* **1999**, *75*, 3932.
[7] M. Terrones, P. M. Ajayan, F. Banhart, X. Blasé, D. L. Carroll, J. C. Charlier, R. Czerw, B. Foley, N. Grobert, R. Kamalakaran, P. Kohler-Redlich, M. Rühle, T. Seeger, H. Terrones, *Appl. Phys. A* **2002**, *74*, 355.
[8] R. Kurt, C. Klinke, J. M. Bonard, K. Kern. A. Karimi, *Carbon* **2001**, *39*, 2163.
[9] R. Kurt, A. Karimi, V. Hoffmann, *Chem. Phys. Lett.* **2001**, *335*, 545.
[10] S. L. Sung, S. H. Tsai, C. H. Tseng, F. K. Chiang, X. W. Liu, H. C. Shih, *Appl. Phys. Lett.* **1999**, *74*, 197.
[11] K. Suenaga, M. P. Jahansson, N. Hellgren, E. Broitman, L. R. Wallenberg, C. Colliex, J. E. Sundgren, L. Hultman, *Chem. Phys. Lett.* **1999**, *300*, 695.
[12] T. Kyotani, L. Tsai, A. Tomita, *Chem. Mater.* **1995**, *7*, 1427.
[13] T. Kyotani, L. Tsai, A. Tomita, *Chem. Mater.* **1996**, *8*, 2109.

Tetramethylpentacene: Remarkable Absence of Steric Effect on Field Effect Mobility**

By *Hong Meng*, *Michael Bendikov*, *Gregory Mitchell*, *Roger Helgeson*, *Fred Wudl*,* *Zhenan Bao*,* *Theo Siegrist*, *Christian Kloc*, and *Cheng-Hsuan Chen*

Substantial progress in pentacene thin-film field-effect transistor (FET) devices has been achieved in the past decade.[1] Organic thin-film FETs have shown charge transport mobilities in the range 0.005–2.1 $cm^2 V^{-1} s^{-1}$ and on/off current ratios larger than 10^8 in some cases.[1] Unlike oligothiophene-based thin-film transistors (TFTs),[2] where an impressive increase in mobility was achieved through the preparation of new semiconductors or by the introduction of new synthetic methodologies, increased performance of pentacene-based TFTs has been mainly achieved through the development of improved device fabrication techniques including:[3] optimization of the film deposition parameters,[3,4] improvement of morphology, dielectric–semiconductor interfacial properties, and purification of materials.[5] While it may be possible to continue the

[*] Prof. F. Wudl, Dr. H. Meng, Dr. M. Bendikov, Dr. G. Mitchell, Dr. R. Helgeson
Department of Chemistry and Biochemistry and Exotic Materials Institute
University of California
Los Angeles, CA 90095-1569 (USA)
E-mail: wudl@chem.ucla.edu
Dr. Z. Bao, Dr. T. Siegrist, Dr. C. Kloc, Dr. C.-H. Chen
Bell Laboratories, Lucent Technologies
600 Mountain Ave, Murray Hill, NJ 07974 (USA)
E-mail: zbao@lucent.com

[**] FW and HM are grateful to the National Science Foundation for support through an IGERT Center (DGE-0114443) and Grant (DMR-9796302), as well as the Air Force (Grant F49620-00-1-0103) and Office of Naval Research (Grant N00014-97-1-0835). Supporting information is available from the authors upon request.

  DOI: 10.1002/adma.200304935

improvement of device performance by employing device physics and engineering techniques, new materials design and synthesis are viable alternatives for pushing pentacene-based TFTs to a new performance level.

There are few examples of pentacene derivatives in the literature[6] and the applications of pentacene derivatives as an active semiconductor layer in TFTs have not been reported. Whereas one could conceive of a number of modified pentacenes through substitution of the hydrogen atoms of the central ring, as was done successfully by Anthony et al.,[6a] we reasoned that substitution of the four terminal hydrogen atoms (the 2, 3 and 9, 10 positions) would be less disruptive while maintaining essentially the intact pentacene nucleus. In this paper our effort has been focused on the modification of the pentacene structure through the introduction of methyl groups in the mentioned 2, 3 and 9, 10 positions, aiming to tune the electronic properties of pentacene with the electron-donating ability and small size of methyl substituents and to study the performance of TFT devices based on these materials.

The multi-step synthesis of 2,3,9,10-tetramethyl-pentacene (Me_4PENT) was performed similarly to the procedures described for pentacene[7] (see supplementary material available from the authors). A cyclization reaction of 4,5-dimethylbenzene-1,2-dicarbaldehyde, obtained by the Swern oxidation of 4,5-dimethylbenzene-1,2-dimethanol,[8] with 1,4-cyclohexanedione gave 2,3,9,10-tetramethyl-pentacene-6,13-dione.[9] The latter was reduced with $Al(Ocy)_3$ (Ocy = cyclohexoxide), prepared in situ by reaction of aluminum foil with a mixture of mercuric chloride and a catalytic amount of carbon tetrachloride in anhydrous cyclohexanol under an argon atmosphere.[10] A high purity sample of Me_4PENT was obtained by two vacuum sublimations.[11]

Me_4PENT is a dark blue solid that is slightly soluble in hot 1,2-dichlorobenzene. Whereas in the solid state Me_4PENT is stable and isolable by sublimation, its solutions are unstable and bleach within 30 min when exposed to air. Thermal analysis of Me_4PENT was performed under nitrogen and, for comparison purposes, pentacene was characterized under similar conditions. The weight loss (due to sublimation) of pentacene began at 260 °C, while that of Me_4PENT started at 340 °C.

Both Me_4PENT and pentacene produce pink solutions in 1,2-diclorobenzene (ODCB) and exhibit a pink-red fluorescence. The longest wavelength band has a characteristic vibronic finger-like shape,[7] and the maxima were slightly red-shifted (by 1–2 nm) in going from pentacene to Me_4PENT (see supporting information).

Cyclic voltammograms of both pentacene and Me_4PENT showed quasi-reversible oxidation and reduction in hot 1,2-dichlorobenzene with n-Bu_4NPF_6 electrolyte. The onset oxidation potentials (E_{oxa}^{onset} vs. saturated calomel electrode (SCE)) and reduction potentials (E_{red}^{onset} vs. SCE) were +0.64 V, –1.34 V for pentacene and +0.51 V, –1.44 V for Me_4PENT, respectively. The bandgaps, determined from the onset oxidation and reduction positions, were 1.98 eV and 1.95 eV for pentacene and Me_4PENT, respectively. The values corresponded well with the calculated highest occupied molecular orbital–lowest unoccupied molecular orbital (HOMO–LUMO) gaps.[12] Thus, the introduction of four weakly electron-donating groups resulted in a significant increase of the HOMO (–4.60 eV for pentacene, –4.41 eV for Me_4PENT) and LUMO energy levels (–2.39 eV for pentacene, –2.18 eV for Me_4PENT) of Me_4-PENT (ca. 0.2 eV), leaving the HOMO–LUMO gaps essentially unchanged at 2.21 eV for pentacene and 2.23 eV for Me_4PENT. These results were consistent with those measured from the onset of UV-vis absorption (ca. 2.06 eV for pentacene and 2.03 eV for Me_4PENT). The high HOMO energy level of Me_4PENT makes it a promising candidate as a hole transporting material in FET devices (see below). On the other hand, it may be more susceptible to oxidation than pentacene.

Highly textured crystalline thin films, as determined by electron diffraction, can be fabricated by vacuum deposition. X-ray diffraction patterns of the thin films also showed strong diffraction peaks with a layer spacing of 16.25 Å, corresponding to the distance between layers of Me_4PENT molecules oriented edge-on on the substrate surface.[13] This kind of molecular orientation is preferred for charge transport since the π–π stacking direction is within the plane of the current flowing direction. Single crystals of Me_4PENT were obtained by the physical vapor transport method using argon as the transport gas as described previously.[11] The crystal structure of Me_4PENT (see Fig. 1) is similar to that of pentacene[14] where the former belongs to a monoclinic and the later to triclinic space group. The unit cell volume of Me_4PENT is 1695 $Å^3$[15] and the tilt angle between two molecular planes is

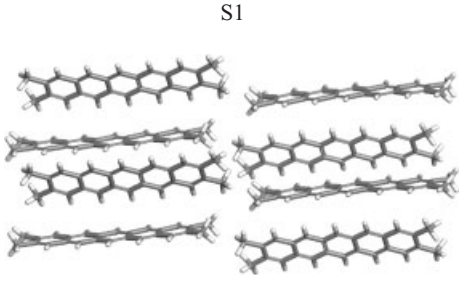

Fig. 1. Crystal structure of Me_4PENT molecules shows the herringbone packing (dark sticks represent C–C bonds and light sticks represents C–H bonds).

53°, compared to 52° in pentacene.[14b] If one considers a pentacene flanked by two other pentacenes in the lattice, the distance between the central pentacene plane and a CH carbon of the central ring (C6) of an adjacent pentacene molecule is 3.43 Å and with the CH carbon of central ring (C13) of the other adjacent molecule it is 3.55 Å. If one considers a Me_4-PENT flanked by two other Me_4PENT in the lattice, the distance between the central Me_4PENT plane and a CH carbon of the central ring (C6) of an adjacent Me_4PENT molecule is 3.58 Å and with the CH carbon of the central ring (C13) of the other adjacent molecule it is 3.72 Å. These observations indicate an apparent minor steric effect by the methyl substituents. Indeed, the methyl–methyl distance in Me_4PENT is 4.272 Å, larger than twice the sum of the van der Waals radii

ADVANCED MATERIALS

of methyl groups (2.0 Å). Due to polymorphism, also observed in pentacene and most molecular solids,[16] the *d*-spacing in thin films is different from that observed in single crystals (17.94 Å). As with pentacene, the Me_4PENT crystal unit cells include two non-equivalent molecules arranged in a herringbone pattern. The overall arrangement of the molecules is not expected to differ radically between the crystal and film structures. The tilt angle of the molecules in reference to surface of the substrate is expected to be smaller, allowing a smaller *d*-spacing than observed in the single crystal.

FET devices were fabricated using two different device geometries: top and bottom contact geometries using gold electrodes.[17] Me_4PENT showed typical p-type FET behavior, indicating that Me_4PENT transports holes. A typical example of a current–voltage (*I–V*) curve is shown in Figure 2. The mobilities were determined in the saturation regime and the results with bottom and top contact device geometries at different substrate deposition temperatures are listed in Table 1.

The mobility value was observed to depend on the substrate deposition temperature. Interestingly, mobilities were higher for the bottom contact mode than for the top contact mode devices fabricated at lower substrate temperatures. The highest mobility was achieved with a bottom contact mode device using a deposition temperature of 85 °C.[18] Even at 22 °C, a mobility of 0.18 $cm^2 V^{-1} s^{-1}$, with a relatively high on/off ratio, was observed. The mobilities achieved in Me_4PENT devices were relatively high, comparable with those for pentacene deposited under similar conditions. The recently reported highest mobility value (ca. 2.1 $cm^2 V^{-1} s^{-1}$) of a pentacene TFT was obtained using surface treatment of the substrates and optimization of the deposition parameters.[16] The commonly measured mobilities of pentacene TFTs (top-contact) are around 0.6 $cm^2 V^{-1} s^{-1}$ for polycrystalline thin films.[1] In addition, a recently reported bottom-contact pentacene-based TFT gave the best value of 0.48 $cm^2 V^{-1} s^{-1}$,[5] a value comparable with our results based on bottom-contact Me_4PENT TFT (0.30 $cm^2 V^{-1} s^{-1}$). Furthermore, all devices were measured in air, which was expected to yield lower on/off ratios due to the fact that an electron-donating-substituted pentacene is expected to react more exothermically with oxygen than pentacene. It should be possible to improve the performance by optimizing the device fabrication processes.

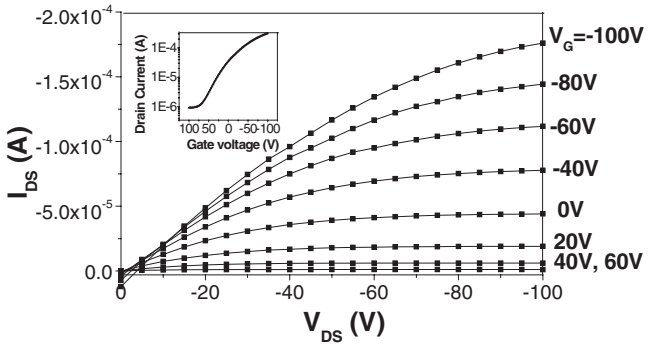

Fig. 2. Drain–source current (I_{DS}) vs. drain–source voltage (V_{DS}) characteristic of a top-contact mode Me_4PENT device at different gate voltages prepared at a substrate temperature of 95 °C with channel length $L = 280$ μm and channel width $W = 4$ mm. Inset: drain–source current (I_{DS}) vs. gate voltage (V_G) characteristic of the same device.

Table 1. Field-effect mobilities and on/off ratios of Me_4PENT at different substrate deposition temperatures.[a,b]

	Room temperature		85 °C		95 °C		105 °C	
	Top	Bottom	Top	Bottom	Top	Bottom	Top	Bottom
Mobility [c] [cm^2/Vs]	0.05	0.18	0.10	0.30	0.20	0.24	0.26	0.12
On/off [d]	2×10^3	1.3×10^3	5.9	6.3×10^3	7×10^2	1.6×10^2	5×10^5	1.9×10^3
V_t [e]	10.0	13.0	72.5	12.5	1.0	1.0	7.0	15.0

[a] For bottom contact (Bottom) the channel width/channel length (W/L) = 250/12 and for top contact (Top), most devices have W/L = 13. In the case of room-temperature, and 85 °C devices, W/L = 29.4 and 14, respectively. [b] The SiO_2 surface was treated with hexamethyldisilazane (HMDS) before evaporation of Me_4PENT. [c] Mobility error is ±0.01 as determined by measuring at least 6 different devices in air. [d] Drain-source current ratio between gate voltage of –100 V and 0 V. This value does not reflect the maximum achievable on/off ratio and is dependent on the interface between the dielectric and semiconducting layer. There is about a 10 % variation between measured devices. [e] The threshold voltage (V_t) error is about a 10 %. V_t is calculated according to the equation $I_{ds} = W/2L[\mu C_i(V_g - V_t)^2]$. The square root of drain source current ($I_{ds}^{1/2}$) is plotted against gate voltage (V_g). The V_g at which the straight line intercepts with the *x*-axis gives the threshold voltage.

Some theoretical publications have previously been devoted to the high mobility of pentacene TFTs.[14a,19] It was proposed that the reorganization energy[20] for self-exchange electron transfer from a charged oligomer to an adjacent neutral oligomer would determine the charge-transport mobility. There are two major parameters that determine self-exchange electron-transfer rates and ultimately charge mobility: i) the electronic coupling between adjacent molecules, which needs to be maximized (pentacene is known for its large electronic coupling between adjacent molecules and X-ray analysis of Me_4PENT has shown that the interlayer distance found in Me_4PENT was similar to that of pentacene);[14a] and ii) the reorganization energy λ, which needs to be small for efficient transport. For pentacene the calculated reorganization energy was remarkably low, which was used to explain the high charge mobility observed in pentacene TFTs.[19]

The calculated vertical ionization potential (IP_v) of Me_4PENT (5.93 eV) was found to be 0.3 eV lower than in pentacene (6.23 eV).[21] Thus, the predicted IP_v of Me_4PENT was 6.2–6.3 eV based on the experimentally measured[19] ionization potential of pentacene, 6.59 eV.

Me_4PENT, like pentacene, is a very rigid molecule and has a very small reorganization energy of only 0.049 eV (about 1.1 kcal/mol).[22] The fact that the reorganization energy of Me_4PENT, with four methyl substituents, was essentially the same as that of pentacene (0.048 eV), was surprising since other known substituted pentacenes were reported to have larger reorganization energies,[19] in contrast to the high mobility measured for Me_4PENT in this work. It is known that mobilities measured in thin films are also strongly dependent on the film morphology. A systematic study of

the effect of morphology on the transistor performance of Me_4PENT is underway and will be reported in a future publication.

In conclusion, a pentacene derivative, Me_4PENT, has been successfully synthesized and single crystals of Me_4PENT were obtained by gradient sublimation. Calculations show that Me_4PENT has similar reorganization energy to that of pentacene. TFTs fabricated with Me_4PENT showed a higher charge transport mobility with the bottom-contact mode device prepared with a deposition substrate temperature of 25 °C and even higher charge transport mobility (0.31 $cm^2 V^{-1} s^{-1}$) in devices prepared with a deposition substrate temperature of 85 °C.

Experimental

2,3,9,10-Tetramethyl-pentacene (Me_4PENT): Into a round-bottomed flask, aluminum wire (2.5 g, 0.093 mol), mercuric chloride (0.05 g, 0.184 mmol), and dry cyclohexanol (100 mL), with one drop of carbon tetrachloride (0.2 mL) were added. The mixture was refluxed overnight under argon. Compound **4** (2,3,9,10-tetramethylpentacene-6,13-dione, supporting information on the synthesis of compound **4** is available from the authors upon request) (1.46 g, 0.004 mol) was then added in one portion and the mixture was refluxed for 3 days. After cooling to 60 °C, the solvent was decanted and ethanol (60 mL) was added. The precipitate was separated by centrifugation, washed with hot acetic acid (2 × 50 mL), 25 % HCl (2 × 50 mL), hot water (2 × 50 mL), and ethanol again (2 × 50 mL). The dark blue compound was dried under vacuum at 60 °C overnight to give a crude product (0.94 g, 70 %), which was further purified by gradient sublimation to yield dark blue crystals m.p. > 300 °C (0.39 g, 42 %). MS (EI) *m/z*: 334 (M^+, 100). HRMS found: 334.1720. Calculated, for $C_{26}H_{22}$, 334.1721. Elemental analysis found: C, 93.61, H, 6.50. Calculated for $C_{26}H_{22}$, C, 93.37, H, 6.63. ^{1}H NMR (ODCB-d_4, 395 K), δ_H 8.72 (s, 2H), 8.35 (s, 4H), 7.52 (s, 4H), 2.31 (s, 12H) ppm. IR (DRIFT, cm^{-1}): 2984 s, 2937 s, 1822 m, 1797 m, 1757 m, 1710 m, 1659 m, 1637 m, 1451 s, 1367 m, 1303 s, 1120 m, 1025 s, 904 s, 873 m.

Received: January 31, 2003
Final version: March 28, 2003

[1] a) C. D. Dimitrakopoulos, D. J. Mascaro, *IBM J. Res. Dev.* **2001**, *45*, 11. b) A. Kraft, *ChemPhysChem* **2001**, *2*, 163. c) H. Klauk, D. J. Gundlach, J. A. Nichols, T. N. Jackson, *IEEE Trans. Electron. Devices* **1999**, *46*, 1258. d) F. Würthner, *Angew. Chem. Int. Ed.* **2001**, *40*, 1037. e) H. Klauk, M. Halik, V. Z. Schieschang, G. Schmid, W. Radlik, W. Weber, *J. Appl. Phys.* **2002**, *92*, 5259.

[2] a) F. Garnier, *Chem. Phys.* **1998**, *227*, 253. b) H. E. Katz, A. Dodabalapur, Z. Bao, in *Handbook of Oligo- and Polythiophenes* (Ed: D. Fichou), Wiley-VCH, Weinheim **1999**, pp. 459–489. c) G. Horowitz, X. Peng, D. Fichou, F. Garnier, *J. Appl. Phys.* **1990**, *67*, 528. d) G. Horowitz, *Adv. Mater.* **1998**, *10*, 365. e) G. Horowitz, R. Hajlaoui, R. B. Bouchriha, M. Hajlaoui, *Adv. Mater.* **1998**, *10*, 923.

[3] Y. Lin, D. J. Gundlach, S. F. Nelson, T. N. Jackson, *IEEE Trans. Electron Devices* **1997**, *44*, 1325.

[4] N. Koch, J. Ghijsen, R. L. Johnson, J. Schwartz, J.-J. Pireaux, A. Kahn, *J. Phys. Chem. B* **2002**, *106*, 4192.

[5] I. Kymissis, C. D. Dimitrakopoulos, S. Purushothaman, *IEEE Trans. Electron Devices* **2001**, *48*, 1060.

[6] a) J. E. Anthony, J. S. Brooks, D. L. Eaton, S. R. Parkin, *J. Am. Chem. Soc.* **2001**, *123*, 9482. b) T. Takahashi, M. Kitamura, B. Shen, K. Nakajima, *J. Am. Chem. Soc.* **2000**, *122*, 12 876.

[7] E. P. Goodings, D. A. Mitchard, G. Owen, *J. Chem. Soc. Perkin Trans. 1* **1972**, 1310.

[8] O. Farooq, *Synthesis* **1994**, 1035.

[9] P. de la Cruz, N. Martin, F. Miguel, C. Seoane, *J. Org. Chem.* **1992**, *57*, 6192.

[10] J. G. Laquindanum, H. E. Katz, A. J. Lovinger, *J. Am. Chem. Soc.* **1998**, *120*, 664.

[11] C. Kloc, P. G. Simpkins, T. Siegrist, R. A. Laudise, *J. Crystal Growth* **1997**, *182*, 416.

[12] Orbital energies for pentacene and Me_4PENT were calculated using density functional theory at B3LYP/6–31G(d)//B3LYP/6–31G(d) level (for discussion of applicability of density functional theory for calculations of orbital energies see: a) E. J. Baerends, O. V. Gritsenko, *J. Phys. Chem. A* **1997**, *101*, 5383. b) R. Stowasser, R. Hoffmann, *J. Am. Chem. Soc.* **1999**, *121*, 3414) using Gaussian 98 series of programs (Gaussian 98, Revision A.7, Gaussian, Inc., Pittsburgh, PA **1998**).

[13] Crystallographic data (excluding structure factors) for the structures reported in this paper have been deposited with the Cambridge Crystallographic Data Center as supplementary publication no. CCDC-196337. Copies of the data can be obtained free of charge on application to CCDC, 12 Union Road, Cambridge CB21EZ, UK (fax: (+44) 1223 336 033; e-mail: deposit@ccdc.cam.ac.uk).

[14] a) J. Cornil, J. P. Calbert, J. L. Brédas, *J. Am. Chem. Soc.* **2001**, *123*, 1250. b) T. Siegrist, C. Kloc, J. H. Schön, B. Batlogg, R. C. Haddon, S. Berg, G. A. Thomas, *Angew. Chem. Int. Ed.* **2001**, *40*, 1732.

[15] The unit cell of Me_4PENT contains four molecules. The unit call volume of pentacene is 686 $Å^3$ and it contains two molecules [14a]. We note that Me_4PENT has four methyl groups and due to the difference in molecular occupation of the unit cell (4 vs. 2) we believe comparison of unit cell volumes may not be very meaningful.

[16] D. J. Gundlach, C.-C. Kuo, S. F. Nelson, T. N. Jackson, in *Dig. 57th Annu. Device Research Conf.*, Santa Barbara, CA, June **1999**, p. 164–165.

[17] H. Meng, Z. Bao, A. J. Lovinger, B. Wang, A. M. Mujsce, *J. Am. Chem. Soc.* **2001**, *123*, 9214.

[18] It is somewhat unusual for bottom-contact devices to have larger mobilities than top-contact devices usually because organic semiconductors tend to form small grains on Au electrodes, resulting in high contact resistance. On the other hand, deposition of metal on organic semiconductors in the top-contact mode may cause damage to the semiconductor and also result in increased contact resistance. In this case, perhaps the grain structure between gold and the organic afforded better contact for bottom-contact devices.

[19] N. E. Gruhn, D. A. da Silva Filho, T. G. Bill, M. Mlagoli, V. Coropceanu, A. Kahn, J. Brédas, *J. Am. Chem. Soc.* **2002**, *124*, 7918.

[20] The reorganization energy (λ) for self-exchange corresponds to the sum of the geometry relaxation energies upon going from the neutral-state geometry to the charged-state geometry and vice versa. These two portions of λ are typically nearly identical, see: M. Malagoli, J. L. Brédas, *Chem. Phys. Lett.* **2000**, *327*, 13.

[21] Adiabatic and vertical ionization energies, as well as the reorganization energy (calculated as the difference between vertical and adiabatic ionization energies), of pentacene and Me_4PENT were calculated using density functional theory (DFT) at the B3LYP/6–31G(d) level using B3LYP/6–31G(d) optimized geometries [12]. The vertical ionization potentials (IP_Vs) were calculated at B3LYP/6–311+G**//B3LYP/6–31G(d).

[22] See supporting information (available from the authors) for details.

Near-Infrared Electroluminescence from Lanthanide Tetraphenylporphyrin:Polystyrene Blends**

By *Tae-Sik Kang*, *Benjamin S. Harrison*, *Timothy J. Foley*, *Alison S. Knefely*, *James M. Boncella*,* *John R. Reynolds*,* and *Kirk S. Schanze**

Several groups have recently demonstrated the application of lanthanide complexes and lanthanide-containing materials in visible and near-IR emitting electroluminescent (EL)

[*] Prof. J. M. Boncella, Prof. J. R. Reynolds, Prof. K. S. Schanze, Dr. T.-S. Kang, Dr. B. S. Harrison, Dr. T. J. Foley, A. S. Knefely
Department of Chemistry and
Center for Macromolecular Science and Engineering
University of Florida
Gainesville, FL 32611-7200 (USA)
E-mail:
boncella@chem.ufl.edu; reynolds@chem.ufl.edu; kschanze@chem.ufl.edu

[**] This work supported by the Defense Advanced Research Projects Agency (Grant No. DAAD 19-00-1-0002).

 DOI: 10.1002/adma.200304692